Journal of Organometallic Chemistry, 225 (1982) 309—329
Elsevier Sequoia S.A., Lausanne — Printed in The Netherlands

SYNTHESIS AND STEREOCHEMICAL ANALYSIS OF THE CUBANE-LIKE $Fe_4(CO)_{12}(\mu_3\text{-}S)_4$ AND $Fe_4(CO)_{12}(\mu_3\text{-}Se)_4$ TETRAMERS: CONVERSION OF THE TETRAMETAL-BONDING Fe_4X_4 CORES IN $Fe_4(NO)_4(\mu_3\text{-}X)_4$ (WHERE X = S, Se) INTO TETRAMETAL-NONBONDING CORES BY SUBSTITUTION OF CARBONYL FOR NITROSYL LIGANDS *

LAWRENCE L. NELSON, FREDERICK YIP-KWAI LO, A. DAVID RAE **, and LAWRENCE F. DAHL *

Department of Chemistry, University of Wisconsin-Madison, Madison, Wisconsin 53706 (U.S.A.)

(Received June 23rd, 1981; in revised form September 2nd, 1981)

Summary

A new series of cubane-like iron-chalcogenide tetramers, $Fe_4(CO)_{12}(\mu_3\text{-}S)_4$ (1) and $Fe_4(CO)_{12}(\mu_3\text{-}Se)_4$ (2), has been prepared and structurally characterized by single-crystal X-ray diffraction. Their synthesis as the major and sole isolated products from the corresponding $Fe_4(NO)_4(\mu_3\text{-}X)_4$ tetramers (X = S, Se) by a high-pressure bomb reaction with CO, in which four nitrosyl ligands are replaced by twelve carbonyl ligands, illustrates a new synthetic route for obtaining cubane-like clusters via addition and/or methathetical reactions. In the formation of these air-stable, insoluble carbonyl tetramers from their nitrosyl precursors, a comparative stereochemical analysis reveals that the idealized cubic $T_d\text{-}\bar{4}3m$ geometry of the central Fe_4S_4 core is unaltered but that the six equivalent Fe—Fe distances greatly enlarge by 0.82 Å from an electron-pair bonding value of 2.65 Å to a nonbonding value of 3.47 Å; for the Fe_4Se_4 core there is a corresponding increase of 0.91 Å in the mean Fe—Fe distance from 2.71 to 3.62 Å. These bond-length changes in the iron-chalcogenide tetramers are completely consistent with a qualitative metal cluster model which predicts that the additional net 12 valence electrons in either 1 or 2 occupy the six empty tetrairon antibonding cluster $(t_1 + t_2)$ MO's of the tetrairon-bonding Fe_4X_4 core in the 60-electron nitrosyl tetramer to give the corresponding tetrairon-nonbonding Fe_4X_4 core in the resulting 72-electron carbonyl tetramer. The concomitant elongation of the Fe—X bonds by 0.11 Å in the

---

* In honor of Professor Henry Gilman for his many years of outstanding research and teaching in the field of organometallic chemistry.

** On leave (December 1979—June 1980) at UW-Madison from School of Chemistry, University of New South Wales, Kensington, NSW, 2033 (Australia).

0022-328X/82/0000—0000/$02.75

Fe_4S_4 core and by 0.10 Å in the Fe_4Se_4 core is attributed to the tetrairon antibonding MO's also possessing significant Fe—X antibonding character. Crystals of 1 are orthorhombic, $Bmmb$, with lattice constants $a = 14.041(4)$, $b = 14.206(3)$, and $c = 10.055(3)$ Å; the calculated density is 2.28 g/cm^3 for $V = 2005.6$ Å^3 and $Z = 4$ with C_{2v}-$mm2$ site symmetry being imposed on each tetramer. Crystals of 2 are tetragonal, $I4_1/amd$, with lattice constants $a = b = 14.312(4)$ Å, $c = 10.141(3)$ Å; the calculated density is 2.80 g/cm^3 for $V = 2077.2$ Å^3 and $Z = 4$ with each tetramer constrained to D_{2d}-$\bar{4}m2$ site symmetry. The crystal structures of both 1 and 2 exhibit essentially identical individual molecular layers (perpendicular to the a axis) which stack by B-centering in 1 and I-centering in 2. This allows for the possibility of stacking faults which, although determined not to be highly significant in the crystal structure of 1, were found to be prevalent in the crystal structure of 2. A method of coping with these particular translational-type, crystal-disorder problems in 1 and 2 via the use of only one additional variable scale factor (in each of these two cases) over that in a conventional, unconstrained least-squares refinement is presented. Refinement with this stacking-fault model incorporated into the least-squares program RAELS gave for 1 $R_1(F) = 4.16\%$, $R_2(F) = 4.88\%$ for 847 independent diffractometry data and for 2 $R_1(F) = 10.70\%$, $R_2(F) = 4.61\%$ for 410 independent diffractometry data (with $R_1(F) = 4.04\%$ for 225 reflections with $I > 2\sigma(I)$).

A qualitative structural-bonding analysis of the presumed cubane-like "tetramethylplatinum" points to its possible existence in that it is an electronically equivalent analog of the cubane-like $Re_4(CO)_{12}(\mu_3\text{-}H)_4$; however, it is concluded from the complete incompatibility between its reported nonbonding Pt—Pt distances vs. expected bonding ones for such an electron-deficient 56-electron system that its true composition is indeed the previously suggested $Pt_4Me_{12}(\mu_3\text{-}OH)_4$.

Introduction

As part of a long-term effort aimed at understanding the relationship between geometry and electronic configuration in cubane-like $[M_4L_{4m}(\mu_3\text{-}X)_4]^n$ clusters [1—3], we are examining their chemical reactivities with various substrates. A major goal is to explore the effects on structure and bonding due to variations in the nature and number of terminal ligands attached to the M_4X_4 core. In particular, we have examined the products formed by reaction of the $[Fe_4(NO)_4(\mu_3\text{-}S)_4]^n$ ($n = 0, -1$) [3,4] and corresponding $[Fe_4(NO)_4(\mu_3\text{-}Se)_4]^n$ ($n = 0, -1$) [5] series with phosphines, methyl and phenyl isocyanides, hexamethylphosphoramide, and carbon monoxide [6]. It was our hope that ligand addition and/or substitution would enlarge the tetrahedral-like ligand environment about each iron without rupture of the Fe_4X_4 core to give new kinds of cubane-like clusters. The net addition of electron-donating ligands to the tetrametal-bonding Fe_4X_4 cores should be electronically feasible since the additional electrons can occupy antibonding tetrairon cluster orbitals thus giving rise to Fe—Fe bond breakage. As predicted, the high-pressure bomb reaction of carbon monoxide with each of the neutral $Fe_4(NO)_4(\mu_3\text{-}X)_4$ clusters did result in the formation of the corresponding $Fe_4(CO)_{12}(\mu_3\text{-}X)_4$ tetramer. In fact, these were the sole products isolated. It is noteworthy that a proposed formulation of $Fe_4(CO)_{12}(\mu_3\text{-}S)_4$ (1) and $Fe_4(CO)_{12}(\mu_3\text{-}Se)_4$ (2) as cubane-like tetramers with cubic T_d symmetry and no metal—metal bonding was made [7] eleven years ago on the basis that such molecular compounds would be electronic and structural analogs of the archetypal $Co_4(CO)_{12}(\mu_3\text{-}Sb)_4$ tetramer.

X-Ray diffraction studies, which were carried out on both **1** and **2** in order to ascertain their presumed tetrameric nature and to elucidate their molecular features, showed the crystal structures to be nonisomorphic. Structural problems involving stacking fault disorders were overcome in each case by the use of the Rae least-squares program, RAELS [8], which enabled the second (minor) crystal-disordered molecular component to be refined as a symmetry-equivalent tetramer via a scale-factor approach. Details of the preparation and structural work are provided in this paper.

These compounds represent the first members of a new series of cubane-like iron-chalcogenide tetramers. Structurally analyzed members of other distinctly different series containing Fe_4S_4, cores include $[Fe_4(\eta^5\text{-}C_5H_5)_4(\mu_3\text{-}S)_4]^n$ (where n = 0 [9,10], —1 [11], —2 [12]), $[Fe_4(SR)_4(\mu_3\text{-}S)_4]^n$ (where R = CH_2Ph, n = —2 [13]; R = Ph, n = —2 [14]; R = $CH_2CH_2CO_2^-$, n = —6 [15]; R = Ph, n = —3 [16,17]; R = CH_2Ph, n = —3 [18]), $[Fe_4Cl_4(\mu_3 - S)_4]^n$ (where n = —2 [19]), $[Fe_4(NO)_4(\mu_3\text{-}S)_4]^n$ (where n = 0 [3,4], —1 [3]), and $[Fe_4(S_2C_2(CF_3)_2)_4(\mu_3\text{-}S)_4]^n$ (where n = —2 [1]). Research in this area has been greatly stimulated by the discovery by Holm, Ibers and coworkers [20] that constituents of the $[Fe_4(SR)_4(\mu_3\text{-}S)_4]^n$ series (n = —1, —2, —3) are analogs of a number of bacterial ferredoxins and high-potential iron proteins (HIPIP) which contain redoxable Fe_4S_4 cores with a cysteinyl ligand attached to each iron atom.

In connection with a comparative structural examination with other cubane-like tetramers [7,21—30] containing transition metals, we also present herein a brief review of the case history of the presumed "tetramethylplatinum" together with our structural-bonding analysis concerning its probable nonexistence. Its preparation was first reported by Gilman and Lichtenwalter [31,32] in 1938, and its solid-state formulation as an electron-deficient cubane-like tetramer, $Pt_4Me_{12}(\mu_3\text{-}Me)_4$, was proposed by Rundle and Sturdivant [27] in 1947 from X-ray diffraction analyses of it and the cubane-like $Pt_4Me_{12}(\mu_3\text{-}Cl)_4$. On the basis that the crystals (supplied by Gilman) of "tetramethylplatinum" were found to be isomorphic with those of the chloride tetramer, Rundle and Sturdivant [27] deduced the methyl positions from the determined heavy-atom platinum positions. The true composition of "tetramethylplatinum" was later questioned [28,33] and extensive evidence was presented [28] that the original compound structurally examined by Rundle and Sturdivant [27] was instead the cubane-like trimethylplatinum hydroxide tetramer, $Pt_4Me_{12}(\mu_3\text{-}OH)_4$ [26,29,30,34,35]. We justify the possible existence of the formulated $Pt_4Me_{12}(\mu_3\text{-}Me)_4$ from qualitative electronic considerations (in its being electronically equivalent to the cubane-like $Re_4(CO)_{12}(\mu_3\text{-}H)_4$ [36—38]), but from the complete incompatibility of such an electronic configuration with the observed nonbonding Pt—Pt distances reported by Rundle and Sturdivant [27] for "tetramethylplatinum" reach the unambiguous conclusion that their crystals were indeed the previously suggested $Pt_4Me_{12}(\mu_3\text{-}OH)_4$.

Experimental

Preparation and physicochemical properties of 1 and 2

All reactions, filtrations, and recrystallizations were carried out under carbon monoxide in standard Schlenk-type glassware. All solvents, which were reagent grade, were dried and distilled over drying agents as follows: toluene (Na; Mallinckrodt Chemical Works) and methanol (MgOMe; Fisher Scientific Co.). The starting compounds $Hg(CN)_2$ (Alfa), $Fe(CO)_5$ (Alfa), and KNO_2 (Fisher Scientific Co.) were used without further purification.

In a typical experiment, 1 was prepared in a Hoke bomb by the reaction of 1.0 g (2.1 mmol) of $Fe_4(NO)_4(\mu_3\text{-}S)_4$ (3) [3,4] in 80 ml of toluene with carbon monoxide (3000 psi) at 80°C for four days. The bomb was then cooled, vented, and opened: removal of the solvent by filtration left behind hundreds of small, shiny black crystals which clung to the walls of the glass liner. Numerous crystals of 2 were analogously obtained by a corresponding high-pressure bomb reaction of 0.40 g (0.61 mmol) of $Fe_4(NO)_4(\mu_3\text{-}Se)_4$ (4) [5] with carbon monoxide under identical conditions. Other than these isolated products and solid starting materials, the bomb reactions gave small amounts of unidentified residues which are presumed to be metallic iron and iron calcogenides.

Crystals of both 1 and 2 are insoluble in common solvents (which thereby precluded spectroscopic measurements in solution) and are not sublimable. Both crystalline compounds also appear to be stable in air for several weaks. These properties are analogous to those previously found [7] for $Co_4(CO)_{12}(\mu_3\text{-}Sb)_4$. Complete elemental analyses (Galbraith Microanalytical Laboratories, Knoxville, Tennessee) of both 1 and 2 provided the following results: 1: Found: Fe, 32.69; S, 18.41, C, 20.82; O, 28.27. for $Fe_4S_4C_{12}O_{12}$ calcd.: Fe, 32.48; S, 18.65; C, 20.96; O, 27.92%; 2: Found: Fe, 25.30; Se, 36.20; C, 16.41; O, 22.16. for $Fe_4Se_4C_{12}O_{12}$ calcd.: Fe, 25.52; Se, 36.09; C, 16.45; O, 21.94%.

Infrared spectra (Beckman 4240 spectrophotometer) of 1 and 2 in KBr-pellet form exhibited similar carbonyl absorption patterns which resembled in overall shape that obtained [7] for $Co_4(CO)_{12}(\mu_3\text{-}Sb)_4$. Three very strong bands at 2070, 2050, and 1998 cm^{-1} and two relatively weak bands at 2023 and 1980 cm^{-1} were measured for 1, while for 2 the corresponding maxima were 2070, 2060, and 2000 cm^{-1} for the three strong bands and 2020 and 1980 cm^{-1} for the two much weaker bands. The expected diamagnetism for each compound was indicated for 1 from room-temperature magnetic measurements. Several attempts to obtain mass spectral data (AEI MS 902C mass spectrometer) on 1 and 2 under a variety of boundary conditions were unsuccessful. Hence, their tetrameric nature was established by single-crystal X-ray diffraction studies.

Preparation of $[Fe_4(CO)_{12}(\mu_3\text{-}X)_4]^+Br^-$ (where X = S, Se)

Since both of these compounds were prepared in an identical fashion, a typical experiment illustrating the preparation of only one of them is given. A 0.22 g (0.32 mmol) sample of 1 was reacted with 0.1 ml (19.5 mmol) of Br_2 in a low-pressure tube under carbon monoxide (30 psi). After being stirred for 15 minutes, the reaction tube was cooled to −68°C in a dry ice-acetone slush and then vented. Following the addition of 80 ml of hexane, the solution was warmed under a CO atmosphere, stirred, recooled to −68°C, and then vented.

Removal of the hexane yielded a brown precipitate which was soluble in polar solvents but which decomposed rapidly if the CO pressure was not maintained.

Prime evidence that this compound was the sought-after bromide salt of the monocation of **1** was given from its infrared spectrum (in chloroform solution) which exhibited a carbonyl band pattern not unlike that of **1** with the corresponding intense peaks of 2110, 2100, and 2050 cm^{-1} being expectedly located at higher frequencies relative to those of the neutral parent. An infrared spectrum of the $[Fe_4(CO)_{12}(\mu_3\text{-}Se)_4]^+Br^-$ analog in $CHCl_3$ was virtually identical to that of the iron-sulfur complex with the three strong terminal carbonyl bands at 2110, 2100, and 2060 cm^{-1}.

Attempts to crystallize each of these salts by a slow solvent diffusion of hexane into a $CHCl_3$ solution of the salt under CO pressure gave rise to either oils or decomposed products. Efforts are presently underway to replace the Br^- ion with other anions such as PF_6^- in the hope of obtaining suitable single crystals for crystallographic analysis.

Single-crystal data collections for 1 and 2

A parallelepiped-shaped crystal of approximate dimensions 0.14 × 0.14 × 0.20 mm for **1** and a cubic-shaped crystal of uniform dimension 0.12 mm for **2** were selected for the crystallographic studies. Each of these crystals was affixed to the end of a glass fiber with epoxy cement and then mounted inside a thin-walled Lindemann glass capillary which was evacuated, filled with argon, and then hermetically sealed. A Syntex (Nicolet) $P\bar{1}$ diffractometer with Mo-K_α radiation was used to obtain intensity data. Details of the crystal alignment and data collection parameters together with a listing of the crystallographic programs (in addition to the ones specifically mentioned herein) are given elsewhere [39]. Intensities were measured once for one reciprocal-lattice octant within the range $3° < 2\theta < 60°$ for **1** and within the range $3° < 2\theta < 40°$ for **2**; for **1** data reduction yielded 847 independent data (corresponding to one octant under orthorhombic D_{2h} Laue symmetry) with 801 reflections having $I > 2\sigma(I)$, while for **2** data reduction gave 410 independent reflections (corresponding to one-half an octant under tetragonal D_{4h} Laue symmetry), of which 225 reflections possessed $I > 2\sigma(I)$. No significant changes in the intensities of the standard reflections were observed during the data collection of either compound. Empirical absorption corrections (based on ψ scans) of the intensities were made for both **1** and **2**.

Crystal data

(a) $Fe_4(CO)_{12}(\mu_3\text{-}S)_4$. Measured lattice constants with estimated standard deviations for the orthorhombic unit cell at ca. 22°C are a = 14.041(4) Å, b = 14.206(3) Å, c = 10.055(3) Å. The unit cell volume of 2005.6 $Å^3$ gives rise to a calculated density of 2.28 g/cm^3 for Z = 4 and f_w = 687.8.

Systematic absences of $\{hkl\}$ for $h + l$ odd and $\{hk0\}$ for k odd indicate the probable space groups to be $Bmmb$ (nonstandard setting of $Cmcm\text{-}D_{2h}^{17}$, no. 63), $Bm2_1b$ (nonstandard setting of $Cmc2_1\text{-}C_{2v}^{12}$, no. 36), or $B2mb$ (nonstandard setting of $Ama2\text{-}C_{2v}^{16}$, no. 40). The conformity of the unit cell to centrosymmetric $Bmmb$ symmetry, which is in accordance with the intensity data closely complying with a centrosymmetric intensity distribution, was subsequently shown from the successful determination and refinement with no unusual distances or bond angles reflecting an incorrect choice. The nonstandard setting of this space group allows a ready comparison with the space group $I4_1/amd$ found for **2** (vide infra). Each of the four molecules per cell is constrained to possess C_{2v}-$mm2$ site symmetry with two Fe atoms, two S atoms, and two CO ligands per tetramer lying on each mirror plane. This corresponds to 16 Fe, 16 S, 16 C and 16 O atoms occupying four sets of 8-fold special positions $8f$ and four sets of 8-fold special positions $8g$. The remaining eight CO ligands per tetramer are in general positions corresponding to 32 C and 32 O atoms occupying four sets of the general 16-fold positions $16h$. With the origin chosen at the center $2/m$, these positions are as follows: $16h$ $(0, 0, 0; 1/2, 0, 1/2) \pm (x, y, z; -x, y, z; x, 1/2 - y, z; -x, 1/2 - y, z)$; 8g $(0, 0, 0; 1/2, 0, 1/2) \pm (x, 1/4, z; \bar{x}, 1/4, z)$ 8f $(0, 0, 0; 1/2, 0, 1/2) \pm (0, y, z; 0, 1/2, - y, z)$. The atomic arrangement in the C_{2v}-constrained tetramer approximates D_{2d}-$\bar{4}m2$ site symmetry with the crystallographic twofold axis being coincident with the pseudo S_4-$\bar{4}$ axis.

(b) $Fe_4(CO)_{12}(\mu_3\text{-}Se)_4$. Lattice constants at ca. 22°C for the determined tetragonal unit cell are $a = b = 14.312(4)$ Å, $c = 10.141(3)$ Å. For $V = 2077.2$ Å^3 and fw = 875.4, the calculated density of 2.80 g/cm^3 for $Z = 4$.

Systematic absences of $\{hkl\}$ for $h + k + l$ odd, $\{hk0\}$ for h and k both odd, and $\{hhl\}$ for $2h + l \neq 4n$ uniquely define the space group $I4_1/amd$-D_{4h}^{19}, no. 141. This centrosymmetric group was verified by the successful structural determination. The similar cell constants and same space group indicate that the crystals of **2** are isomorphic with those of $Co_4(CO)_{12}(\mu_3\text{-}Sb)_4$. The 16 Fe and 16 S atoms occupy two sets of 16-fold special positions $16h$ on minor planes, while the 48 C and 48 O atoms each occupy one set of the general 32-fold positions $32i$ and one set of $16h$. Based on the origin being chosen at the center $2/m$ located at $0, -1/4, 1/8$ from $\bar{4}m2$, these coordinates are as follows: $32i$ $(0, 0, 0; 1/2, 1/2, 1/2) \pm (x, y, z, -x, y, z; x, 1/2 - y, z; -x, 1/2 - y, z; 1/4 - y, 1/4 - x, 3/4 - z; 3/4 + y, 1/4 - x, 3/4 - z; 1/4 - y, 1/4 + x, 3/4 - z; 3/4 + y, 1/4 + x, 3/4 - z)$; $16h$ $(0, 0, 0; 1/2, 1/2, 1/2) \pm (0, y, z; 0, 1/2 - y, z; 1/4 + x, 1/4, 3/4 + z; 3/4 - x, 1/4, 3/4 + z)$. The eight equivalent positions listed inside the second brackets in set $32i$ create a $Fe_4(CO)_{12}(\mu_3\text{-}Se)_4$ tetramer of D_{2d}-$\bar{4}m2$ site symmetry at $0, 1/4, -1/8$; the first four equivalent positions are the same as those listed previously for set $16h$ in $Bmmb$. These similarities are consistent with the atomic arrangement in the iron-selenium tetramer being analogous to that in the iron-sulfur tetramer except that now D_{2d}-$\bar{4}m2$ symmetry is strictly imposed.

Structural determinations and refinements

In all structure factor calculations on both compounds anomalous dispersion corrections [40] were applied to the scattering factors of all atoms.

(a) $Fe_4(CO)_{12}(\mu_3\text{-}S)_4$. Initial efforts to solve the crystal structure of **1** by application of MULTAN 76 [41] to each of the three previously-mentioned possible space groups were unsuccessful. In these cases where the automatic solution of the phase problem via the MULTAN program failed, no attempt was made to modify the boundary conditions (e.g., select new origin and starting phases and/or vary the number of interactions present). Instead, the crystal structure of **1** was determined from an interpretation of a computed

Patterson synthesis. This analysis was based upon the known atomic parameters [7] of $Co_4(CO)_{12}(\mu_3\text{-}Sb)_4$ coupled with those of the structurally related $Fe_4(CO)_{12}(\mu_3\text{-}Se)_4$. The Patterson peaks in 1 were consistent with a B-centering of a layer in the *bc* plane of two $Fe_4(CO)_{12}(\mu_3\text{-}S)_4$ molecules per cell. This single layer of $Fe_4(CO)_{12}(\mu_3\text{-}S)_4$ molecules is effectively identical to that found for the packing of the $Fe_4(CO)_{12}(\mu_3\text{-}Se)_4$ molecules in its body-centered crystal structure (vide infra). Hence, the nonisomorphic structures of 1 and 2 differ only in the stacking of layers perpendicular to the *a* axis. The essential similarity of a single layer in the two structures reinforced the crystallographic evidence encountered in 2 for the possible occurrence of stacking faults (vide infra). In order to allow for this possibility in 1, $\{hkl\}$ data with $k = 2n + 1$ were given one refineable scale factor, K_1, while $\{hkl\}$ data with $k = 2n + 1$ were given a second scale parameter, K_2. Refinement was performed with the least-squares program RAELS [8] with slack constraints [42,43] being utilized in the initial cycles on the differences (ideally zero) between Fe—C bonds, the differences (ideally zero) between C—O bonds, and the Fe—C—O bond angles (ideally 180°). Under these constraints (for which average discrepancies were: Fe—C, 0.002 Å; C—O, 0.001 Å; Fe—C—O, 1.2°), discrepancy factors of $R_1(F) = [\Sigma||F_o| - |F_c||/\Sigma|F_o|] \times 100 = 4.20\%$ and $R_2(F) = [\Sigma w_i||F_o| - |F_c||^2/w_i|F_o|^2]^{1/2} \times 100 = 4.93\%$ were obtained for the anisotropic refinement [8] of all 847 data. Upon removal of these constraints, the refinement of the resulting 86 parameters converged at $R_1(F) = 4.16\%$, $R_2(F) = 4.88\%$; scale factors of $K_1 = 0.674(2)$ and $K_2 = 0.639(2)$ with $\Delta K = 0.035(4)$ were obtained. The a_2/a_1 ratio of the occupancy factor a_2 for the minor component (related by a *I*-centered disorder) relative to the occupancy factor for the predominant component (of *Bmmb* symmetry) is estimated from $a_2/a_1 = (K_1 - K_2)/(K_1 + K_2)$ (see appendix) to be 0.035/1.313, which corresponds to normalized values of $a_1 = 0.973$ and $a_2 = 0.027$. The validity of this stacking-fault model (which involves the use of two variable scale factors K_1 and K_2) may be readily seen from a comparison of the corresponding discrepancy indices obtained from a conventional unconstrained refinement (with one variable scale factor). The resulting 85 parameters in this latter refinement gave significantly higher $R_1(F)$ and $R_2(F)$ values of 4.53% and 5.34%, respectively, with the single scale parameter of $K = 0.663$ for the 847 independent reflections. However, the small a_2/a_1 ratio indicates that the crystal of 1 examined by X-ray diffraction contains relatively few stacking faults.

A comparison of the final cycles for the two unconstrained refinements (with one and two scale parameters) revealed no significant differences between corresponding positional and thermal atomic parameters. Those from the output of the last cycle of the unconstrained refinement with two scale factors are given in Table 1, while interatomic distances and bond angles are given in Table 2. A final Fourier difference map exhibited no unusual features. Observed and calculated structure factors are listed in the supplementary material.

(b) $Fe_4(CO)_{12}(\mu_3\text{-}Se)_4$. Atomic coordinates from the indicated isomorphous $Co_4(CO)_{12}(\mu_3\text{-}Sb)_4$ structure [7] were used as initial coordinates for the corresponding atoms in 2. However, difficulties were encountered in attempted least-squares refinements of 2 with the OR FLS program [44]. In particular, the atomic anisotropic thermal coefficients for C(1) and O(1) refined to physically meaningless values. A three-dimensional Fourier difference map revealed the

TABLE 1

ATOMIC PARAMETERS FOR $Fe_4(CO)_{12}(\mu_3\text{-}S)_4$ [a]

A. Atomic positional parameters [b]

Atom	x	y	z
Fe(1)	0.12380(7)	1/4(—)	—0.00294(15)
Fe(2)	0(—)	0.37238(8)	—0.24259(13)
S(1)	0(—)	0.35831(14)	—0.01212(26)
S(2)	0.1101(1)	1/4(—)	—0.23358(26)
C(1)	0.1198(6)	1/4(—)	0.1768(12)
O(1)	0.1190(5)	1/4(—)	0.2898(8)
C(2)	0.2141(4)	0.3416(4)	—0.00776(8)
O(2)	0.2725(3)	0.3972(3)	—0.00967(7)
C(3)	0(—)	0.3724(7)	—0.4214(11)
O(3)	0(—)	0.3758(6)	—0.5350(8)
C(4)	0.0931(4)	0.4614(5)	—0.2314(7)
O(4)	0.1493(3)	0.5181(3)	—0.2246(2)

B. Anisotropic thermal factors ($\times 10^3$) [a, b]

Atom	U_{11}	U_{22}	U_{33}	U_{12}	U_{13}	U_{23}
Fe(1)	17(0)	24(0)	25(0)	0(—)	—2(0)	0(—)
Fe(2)	19(0)	26(0)	29(0)	0(—)	0(—)	2(0)
S(1)	21(0)	23(1)	29(1)	0(—)	0(—)	0(1)
S(2)	20(1)	29(1)	31(1)	0(—)	3(1)	0(—)
C(1)	22(5)	24(5)	59(7)	0(—)	—6(4)	0(—)
O(1)	49(4)	62(5)	38(4)	0(—)	4(3)	0(—)
C(2)	25(2)	32(3)	32(3)	5(2)	2(3)	1(3)
O(2)	37(2)	39(2)	74(3)	—17(2)	0(3)	—2(3)
C(3)	27(5)	24(5)	38(6)	0(—)	0(—)	—1(4)
O(3)	52(4)	71(6)	47(5)	0(—)	0(—)	—1(4)
C(4)	33(3)	28(3)	32(3)	3(2)	3(3)	3(3)
O(4)	38(2)	48(3)	64(3)	—18(2)	3(2)	—2(2)

[a] Estimated standard deviations of the last significant figures are given in parentheses for this and the following tables. [b] The anisotropic thermal parameters are of the form $\exp[-2\pi^2(U_{11}h^2a^{\star 2} + U_{22}k^2b^{\star 2} + U_{33}l^2c^{\star 2} + 2U_{12}hka^{\star}b^{\star} + 2U_{13}hla^{\star}c^{\star} + 2U_{23}klb^{\star}c^{\star})]$ where U_{ij} represents the thermal parameter expressed in terms of mean-square amplitudes of vibrations.

nature of the problem. The structure appeared to be disordered with a Se atom of a ghosted tetramer lying midway between the independent C(1) and O(1) atoms located on a mirror plane. A knowledge of the structure of $Fe_4(CO)_{12}(\mu_3\text{-}S)_4$ prompted the idea that the disorder arose from an occasional B-centered stacking of layers perpendicular to the *a* direction rather than the usual body-centered stacking. The stacking operation $E(1/2, 0, 1/2) + (\theta, t)$ (where $E(1/2, 0, 1/2)$ is the B-centered stacking fault and $(\theta, t) = 1/4 + y$, $1/4 + x$, $3/4 + z$ is a symmetry element of $I4_1/amd$) acting on the Se atom located approximately at 0, 3/8, 0 produces a ghost at 1/8, 1/4, 1/4 midway between C(1) and O(1). This crystal disorder, if regarded as the consequence of a translational displacement of the tetrameric structure by simple 1/2-cell fractional coordinates, can be described by the use of different scale constants for data of different *hkl* index conditions. The methodology for this way of correcting for a stacking fault is outlined in the appendix of this paper. The $h = 2n$, $k = 2n$, $l = 2n$ data for 2 are unchanged by the existence of stacking faults, but data of other index conditions become weaker in intensity. Failure to

TABLE 2

INTRAMOLECULAR DISTANCES AND BOND ANGLES FOR $Fe_4(CO)_{12}(\mu_3\text{-}S)_4$ [a]

A. Distances (Å) averaged under cubic T_d symmetry			
Fe(1)···Fe(1′)	3.477(2)	S(1)···S(1′)	3.078(4)
Fe(2)···Fe(2′)	3.477(2)	S(2)···S(2′)	3.093(4)
Fe(1)···Fe(2)	3.443(2)	S(1)···S(2)	3.118(3)
	3.466(av)		3.096(av)
Fe(1)—S(1)	2.326(3)	Fe(1)—C(1)	1.823(7)
Fe(1)—S(2)	2.329(2)	Fe(1)—C(2)	1.799(11)
Fe(2)—S(1)	2.324(2)	Fe(2)—C(3)	1.817(6)
Fe(2)—S(2)	2.328(3)	Fe(2)—C(4)	1.809(12)
	2.327(av)		1.812(av)
C(1)—O(1)	1.139(7)		
C(2)—O(2)	1.136(12)		
C(3)—O(3)	1.130(7)		
C(4)—O(4)	1.143(11)		
	1.137(av)		
B. Bond angles (deg) averaged under cubic T_d symmetry			
S(1)—Fe(1)—S(1)′	83.2(1)	Fe(1)—S(1)—Fe(1′)	96.9(1)
S(2)—Fe(2)—S(2′)	83.0(1)	Fe(2)—S(2)—Fe(2′)	96.0(1)
S(1)—Fe(1)—S(2)	84.1(1)	Fe(1)—S(1)—Fe(2)	95.5(1)
S(1)—Fe(2)—S(2)	84.2(1)	Fe(1)—S(2)—Fe(2)	95.4(1)
	83.6(av)		96.0(av)
C(1)—Fe(1)—C(2)	93.5(3)	Fe(1)—C(1)—O(1)	178.1(5)
C(3)—Fe(2)—C(4)	92.8(3)	Fe(1)—C(2)—O(2)	178.8(9)
C(2)—Fe(1)—C(2″)	92.3(4)	Fe(2)—C(3)—O(3)	178.5(6)
C(4)—Fe(2)—C(4″)	91.5(4)	Fe(2)—C(4)—O(4)	177.6(9)
	92.5(av)		178.3(av)
S(1)—Fe(1)—C(1)	89.9(2)	S(1)—Fe(1)—C(2)	175.1(3)
S(1)—Fe(1)—C(2″)	91.0(2)	S(1)—Fe(2)—C(3)	174.3(3)
S(1)—Fe(2)—C(4)	92.8(2)	S(2)—Fe(1)—C(1)	172.8(2)
S(2)—Fe(2)—C(3)	92.3(2)	S(2)—Fe(2)—C(4)	173.5(3)
S(2)—Fe(2)—C(4″)	92.2(2)		
S(2)—Fe(1)—C(2)	92.2(2)		173.9(av)
	91.7(av)		

[a] The primed atoms denote those related by the crystallographic twofold axis, while the doubly primed atoms denote those related by one of the two crystallographic vertical mirror planes.

model this type of disorder leads to systematic error, the instance detailed above for **2** being the most important. We have described only the B-centered fault in $I4_1/amd$; from symmetry considerations, A-centered faults can also occur within different mosaic components of a crystal. By a merging of the $|F(hkl)|^2$ and $|F(khl)|^2$ data (which are equivalent under the indicated D_{4h} Laue symmetry) in the data reduction, the crystal structure (which thereby must possess both A- and B-centered faults) was refined [45] with RAELS

[8] by the use of three distinct scale factors (viz., K_1 for $\{hkl\}$ data with $h = 2n$, $k = 2n$, $l = 2n$; K_2 for $\{hkl\}$ data with $h = 2n + 1$, $k = 2n + 1$, $l = 2n$; and K_3 for $\{hkl\}$ data with $h + k = 2n + 1$, $l = 2n + 1$). (Data associated with K_3 would have two separate associated K values had data merging not been used to put the $|F(hkl)|^2$ and $|F(kh)|^2$ data on the exact same scale).

Electron density maps for the ordered structure were obtained by a multiplication of the observed $|F_0|$ data by the reciprocal of the appropriate scale factor. Initial refinement was carried out with three independent scale factors and with the following slacks constraints [42,43] being imposed on the badly behaved carbonyl ligand: viz., C—O and Fe—C bond lengths equal to those for the other independent CO ligand and Fe—C—O bond angles of 180°. This refinement with three independent scale factors converged at an overall $R_1(F)$ index of 4.08% for the three classes of 225 observed data (with $I > 2\sigma(I)$). The $R_1(F)$ values associated with the individual classes (K_1, K_2, and K_3) were 2.64, 10.40, and 5.95%, respectively. Values of $K_1 = 0.488(1)$, $K_2 = 0.223(7)$ and $K_3 = 0.401(4)$ were obtained. The much smaller value of K_2 relative to those of K_1 and K_3 indicated that eq. 1 in the appendix could not be meaningfully interpreted. Since there are only 20 independent observed reflections with this index condition and as it was already known that the B-centered stacking fault causes a ghosted Se atom to interfere with the refinement of one carbonyl ligand, it was thereby decided to constrain K_1, K_2, and K_3 such that $K_3^2 = (K_1^2 + K_2^2)/2$ (see Appendix). This was done with RAELS [8] via the method of Busing [46]. The resulting final refinement with two independent variables K_1 and K_2 changed the scale factors to $K_1 = 0.490(3)$ and $K_2 = 0.245(1)$, for which $K_3 = 0.387$; the overall $R_1(F)$ index for the three classes of 225 observed data (with $I > 2\sigma(I)$) was 4.04% with R_1 values of 2.50, 10.81, and 5.90% being obtained for the individual classes of observed data associated with K_1, K_2, and K_3, respectively. The corresponding overall $R_1(F)$ and $R_2(F)$ values for all 410 independent reflections (i.e., including those with $I \leqslant 2\sigma(I)$) were 10.70% and 4.61%, respectively. The a_2/a_1 ratio for the occupancy factors, where a_2 is the occupancy factor for the disordered component (A- and B-centering disorder) and a_1 the occupancy factor for the nondisordered component of $I4_1/amd$ symmetry, is estimated from $a_2/a_1 = (K_1 - K_2)/(K_1 + K_2)$ (see Appendix) to be 0.245/0.735. The resulting normalized values of $a_1 = 0.750$ and $a_2 = 0.250$ indicate a considerable occurrence of stacking faults in the crystal structure of 2. An examination of the last cycle of this refinement showed for the above-mentioned slack constraints that the difference between the two independent C—O bonds held to 0.003 Å, the difference between two independent Fe—C bonds held to 0.002 Å, while the constrained linearity of the two independent Fe—C—O bond angles held to 1.1 and 1.2°; it is noteworthy that these internal coordinate differences are included as residuals in the least-squares process [45] utilized in RAELS [8]. A final Fourier difference map showed no anomalous features.

Final atomic parameters for 2 are presented in Table 3, while interatomic distances and bond angles are given in Table 4. The estimated standard deviations for the Fe—C and C—O bond lengths are more realistically those of the mean Fe—C and C—O distances whose values were not constrained in any way. The correctness of the crystal-disordered model (relative to the initial crystal-

TABLE 3

ATOMIC PARAMETERS FOR $Fe_4(CO)_{12}(\mu_3\text{-Se})_4$

A. Atomic positional parameters

Atom	x	y	z
Fe	0.1279(1)	1/4(—)	−0.0004(4)
Se	0(—)	0.3636(1)	−0.0096(4)
C(1)	0.1268(6)	1/4(—)	0.1748(12)
O(1)	0.1254(12)	1/4(—)	0.2908(10)
C(2)	0.2136(6)	0.3397(7)	−0.0101(22)
O(2)	0.2701(6)	0.3994(5)	−0.0183(21)

B. Anisotropic temperature factors (X 10^3)

Atom	U_{11}	U_{22}	U_{33}	U_{12}	U_{13}	U_{23}
Fe	29(1)	28(1)	29(1)	0(—)	0(2)	0(—)
Se	25(0)	23(0)	22(1)	0(—)	0(—)	−2(1)
C(1)	30(12)	45(13)	25(9)	0(—)	−4(8)	0(—)
O(1)	79(15)	66(12)	12(7)	0(—)	−15(7)	0(—)
C(2)	37(5)	38(5)	26(6)	5(4)	11(9)	−1(9)
O(2)	44(6)	56(4)	67(9)	−8(4)	−9(7)	−2(7)

TABLE 4

INTRAMOLECULAR DISTANCES AND BOND ANGLES FOR $Fe_4(CO)_{12}(\mu_3\text{-Se})_4$ [a]

A. Distances (Å) averaged under cubic T_d symmetry

Fe···Fe′	3.617(6)	Se···Se′	3.252(4)
Fe···Fe″	3.617(6)	Se···Se″	3.281(6)
	3.617(av)		3.267(av)
Fe—Se	2.450(2)	Fe—C(1)	1.778(12)
Fe—Se″	2.442(6)	Fe—C(2)	1.779(10)
	2.446(av)		1.778(av)
		C(1)—O(1)	1.176(14)
		C(2)—O(2)	1.179(13)
			1.178(av)

B. Bond angles (deg) averaged under cubic T_d symmetry

Se—Fe—Se′	83.2(1)	Fe—Se—Fe′	95.4(1)
Se—Fe—Se″	84.2(1)	Fe—Se—Fe″	96.7(1)
	83.7(av)		96.0(av)
Cl—Fe—C(2)	93.5(8)	Fe—C(1)—O(1)	178.9(7)
C(2)—Fe—C(2′)	93.5(8)	Fe—C(2)—O(2)	179.8(8)
	93.5(av)		179.3(av)
Se—Fe—C(1)	91.8(3)	Se—Fe—C(2′)	175.2(5)
Se—Fe—C(2)	92.0(2)	Se″—Fe—C(1)	174.7(5)
Se″—Fe—C(2)	91.8(2)		
			175.0(av)
	91.9(av)		

---

[a] The primed atoms denote those related by one of the two crystallographic vertical mirror planes, while the doubly primed atoms denote those related by the crystallographic S_4-$\bar{4}$ axis.

ordered model) is evidenced not only by the reasonable $R_1(F)$ and $R_2(F)$ indices but also more impressively by the resulting sensible atomic thermal parameters (unconstrained) and by the resulting conformity of the molecular parameters for the Fe_4Se_4 core to cubic T_d symmetry with normal values. Observed and calculated structure factors are given as supplementary material, please refer to the authors to obtain information.

Results and discussion

Crystal and molecular descriptions of $Fe_4(CO)_{12}(\mu_3\text{-}S)_4$ (1) and $Fe_4(CO)_{12}(\mu_3\text{-}Se)_4$ (2)

Both **1** and **2** consist of tetrameric molecules in which four $Fe(CO)_3$ fragments positioned at the corners of a regular nonbonding tetrahedron are interconnected by face-bridging chalcogenide atoms. The overall geometry of the resulting Fe_4X_4 core is that of a distorted cube. The three terminal carbonyl ligands and three chalcogenide atoms form a trigonally distorted octahedral-like arrangement about each iron atom. Both of the molecular configurations for 1 (Fig. 1) of crystallographic C_{2v}-$mm2$ site symmetry and for **2** (Fig. 2) of crystallographic D_{2d}-$\bar{4}m2$ site symmetry conform closely to cubic T_d-$\bar{4}3m$ symmetry.

The crystal structures of **1** and **2**, which possess a common layer (perpendicular to the *a* axis) of two molecules per cell, differ from each other in whether the adjacent layers are related to the common one by either B-centering (as found in **1**) or I-centering (as found in **2**). The particular crystals utilized in the structural determinations exhibited evidence of translational disorder in the stacking of the layers; hence, a stacking fault model was utilized in the successful refinement of each structure. An examination of the crystal packing of **1** and **2** reveals no unusual features which might account for the general insolubility of these compounds as well as that of $Co_4(CO)_{12}(\mu_3\text{-}Sb)_4$. The closest intermolecular separations (viz., O···O contact distances) of 2.88 Å in **1** and 2.95 Å in **2** indicate that the crystalline interactions are mainly of Van der Waals type. It is noteworthy that $Fe_2(CO)_9$ [47] is another example of a molecular solid-state compound with is also generally insoluble in solvents with which it does not react.

Comparative relationship of 1 and 2 with other $M_4(CO)_{12}(\mu_3\text{-}X)_4$ tetramers

These iron-chalcogenide tetramers are two additional members of the widely occurring cubane-like $M_4(CO)_{12}(\mu_3\text{-}X)_4$ tetramers. Other members whose solid-state structures have been ascertained by X-ray diffraction include $Co_4(CO)_{12}(\mu_3\text{-}Sb)_4$ [7], $Os_4(CO)_{12}(\mu_3\text{-}O)_4$ [21], $Re_4(CO)_{12}(\mu_3\text{-}F)_4 \cdot 4\ H_2O$ [22], $Fe_4(CO)_{12}(\mu_3\text{-}AsMe)_4$ [23], $Mn_4(CO)_{12}(\mu_3\text{-}F)_2(\mu_3\text{-}OH)_2 \cdot 2\ C_6H_6$ [24], and $Re_4(CO)_{12}(\mu_3\text{-}SMe)_4$ [25]. All of these diamagnetic tetramers as well as the electronically equivalent and structurally similar $Mo_4\{(NO)(CO)_2\}_4(\mu_3\text{-}OH \cdot OPPh_3)_4$ [48], $Co_4(\eta^5\text{-}C_5R_5)_4(\mu_3\text{-}X)_4$ (where R = H, X = S [49], Te [50]; R = Me, X = Te [50]), and $Ni_4(\eta^5\text{-}C_5H_5)_4(\mu_3\text{-}P)_4$ [51] possess octahedrally coördinated metal atoms (i.e., based on the cyclopentadienyl ligand being regarded as tri-

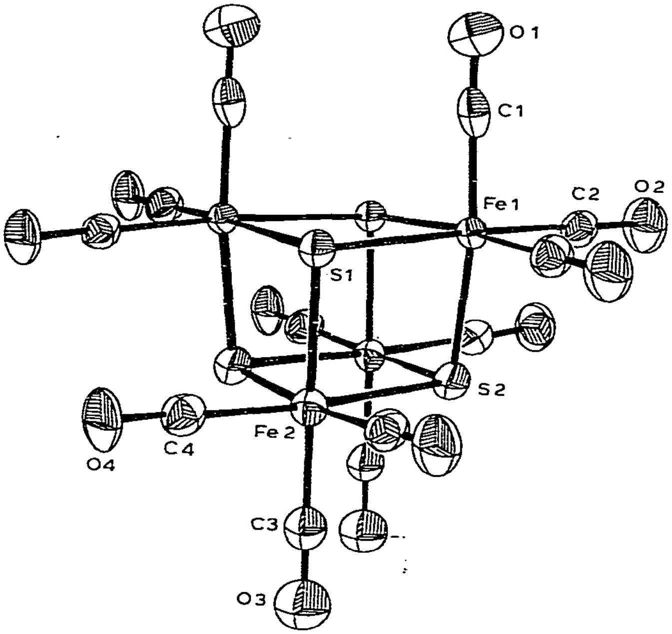

Fig. 1. View of the $Fe_4(CO)_{12}(\mu_3\text{-}S)_4$ molecule of idealized cubic T_d-$\overline{4}3m$ geometry and crystallographic C_{2v}-$mm2$ site symmetry.

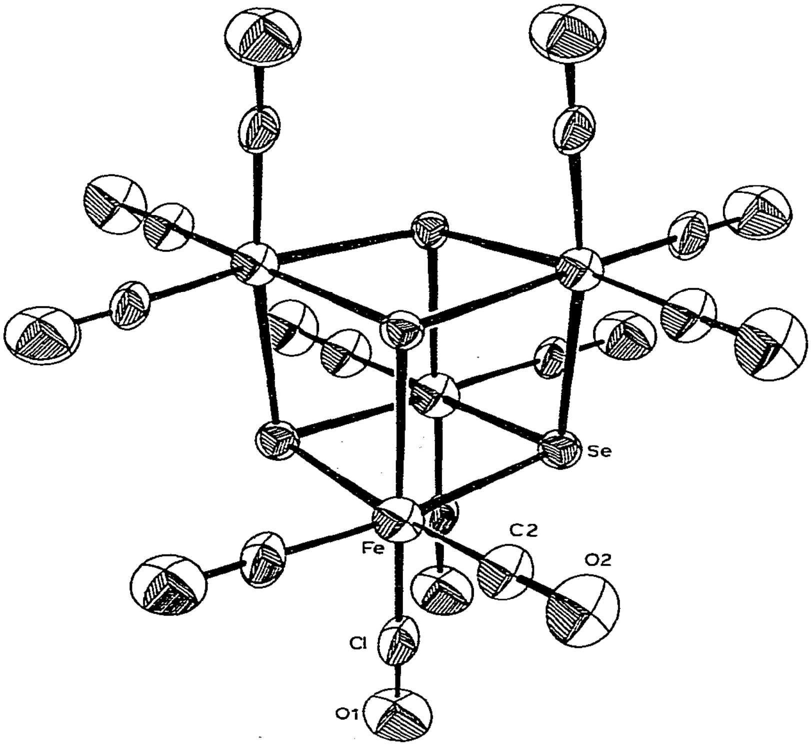

Fig. 2. View of the $Fe_4(CO)_{12}(\mu_3\text{-}Se)_4$ molecule of idealized cubic T_d-$\overline{4}3m$ geometry and crystallographic D_{2d}-$\overline{4}m2$ site symmetry.

dentate) of d^6 formal oxidation state with nonbonding metal—metal distances in accordance with no direct metal—metal bonding *.

Comparative structural-bonding relationship of 1 and 2 with their cubane-like $Fe_4(NO)_4(\mu_3\text{-}X)_4$ precursors ($X = S$ (3), Se (4))

Of prime interest are the geometrical changes determined in the cubic T_d Fe_4X_4 cores (X = S, Se) upon the substitution of twelve carbonyl ligands in place of the four nitrosyl ones. Table 5 reveals that for the Fe_4S_4 core the six equivalent Fe—Fe distances greatly enlarge by an average value of 0.82 Å from an electron-pair bonding value of 2.65 Å in **3** to a nonbonding value of 3.47 Å in **1**, while for the Fe_4Se_4 core there is a corresponding increase of 0.91 Å from 2.71 in **4** to 3.62 Å in **2**. The other prominent bond-length expansion in the Fe_4S_4 core is a significant 0.11 Å lengthening in the twelve Fe—S bonds from 2.22 Å in **3** to 2.33 Å in **1**. An analogous 0.10 Å lengthening from 2.35 in **4** to 2.45 Å in **1** occurs in the twelve Fe—Se bonds of the Fe_4Se_4 core. This concomitant elongation of the Fe—X bonds upon expansion of the Fe—Fe bonds may be readily attributed to electronic effects which suggests that the tetrairon antibonding cluster orbitals also possess significant Fe—X antibonding character. A similar direct correlation between Fe—Fe and Fe—S distances has been previously noted [9—12] within the Fe_2S_2 fragments of the Fe_4S_4 cores in the $[Fe_4(\eta^5\text{-}C_5H_5)_4(\mu_3\text{-}S)_4]^n$ series (n = 0, +1, +2).

The iron-chalcogenide carbonyl tetramers provide an operational test of the qualitative molecular orbital cluster model [54—56] which has been utilized to describe the electronic configurations and resultant metal—metal bonding in a variety of cubane-like M_4X_4 clusters and which has clearly distinguished [4] the different electronic configurations for three other dissimilar Fe_4S_4 cluster series viz., $[Fe_4(NO)_4(\mu_3\text{-}S)_4]^n$ (n = 0, —1), $[Fe_4(\eta^5\text{-}C_5H_5)_4(\mu_3\text{-}S)_4]^n$ (n = 0, +1, +2), and $[Fe_4(SR)_4(\mu_3\text{-}S)_4]^n$ (n = —1, —2, —3). This qualitative bonding description, which has been substantiated for these cubane-like systems by quantitative calculations [57] via application of the Fenske-Hall MO model [58], assumes for the neutral $Fe_4(NO)_4(\mu_3\text{-}X)_4$ tetramers (X = S, Se) that each iron formally possesses a d^7 Fe^I configuration by its coordination with a NO^+ ligand and three triply bridging X^{2-} ligands. The resulting 28 available iron core electrons from the four equivalent d^7 Fe^I atoms produce under cubic T_d symmetry the ground state $(e + t_1 + t_2)^{16}(a_1 + e + t_2)^{12}(t_1 + t_2)^0$, in which the six tetrairon bonding cluster orbitals $(a_1 + e + t_2)$ are completely filled and the six higher-energy tetrairon antibonding cluster orbitals $(t_1 + t_2)$ are empty. In this case the eight $(e + t_1 + t_2)$ tetrairon orbitals, which are not involved in direct Fe—Fe interactions and hence which are nonbonding relative to direct

---

* A structurally proven exception of a $M_4(CO)_{12}(\mu_3\text{-}X)_4$ tetramer with no M—M bonds is $Re_4(CO)_{12}$-$(\mu_3\text{-}InRe(CO)_5)_4$ [52] whose central Re_4In_4 framework containing four equivalent d^3 Re^{IV} possesses a completely bonding tetrarhenium tetrahedron with a mean Re—Re electron-pair distance of 3.028(5) Å. In contrast, there are a considerable number of examples of cubane-like $M_4(\mu^5\text{-}C_5R_5)_4(\mu_3\text{-}X)_4$ tetramers containing M—M bonds [9—12,49,50,51,53].

TABLE 5

SELECTED MEAN DISTANCES (Å) AND BOND ANGLES (deg) FOR THE PSEUDO-CUBIC T_d Fe_4X_4 CORES IN THE $Fe_4(CO)_{12}(\mu_3\text{-}X)_4$ TETRAMERS (X = S, Se) AND IN THEIR CHEMICAL PRECURSORS, $Fe_4(NO)_4(\mu_3\text{-}X)_4$ (X = S, Se)

Tetramer	$Fe_4(NO)_4$-$(\mu_3\text{-}S)_4$ (3)	$Fe_4(CO)_{12}$-$(\mu_3\text{-}S)_4$ (1)	Difference $\Delta(1-3)$	$Fe_4(NO)_4$-$(\mu_3\text{-}Se)_4$ (4)	$Fe_4(CO)_{12}$-$(\mu_3\text{-}Se)_4$ (2)	Difference $\Delta(2-4)$
Reference	3, 4	This work		5	This work	
Crystallographic site symmetry	C_i-$\bar{1}$	C_{2v}-$mm2$		C_i-$\bar{1}$	D_{2d}-$\bar{4}m2$	
Fe—Fe	2.651	3.466	0.815	2.705	3.617	0.912
X···X	3.503	3.096	−0.407	3.835	3.267	−0.568
Fe—X	2.217	2.327	0.110	2.349	2.446	0.097
Fe—X—Fe	73.4	96.0	22.6	70.3	96.0	25.7
X—Fe—X	104.4	83.6	−20.8	106.6	83.7	−22.9

tetrairon interactions, have been found from quantitative (Fenske-Hall)-type MO calculations [57] on $Fe_4(NO)_4(\mu_3\text{-}S)_4$ to be at lower energies than the six tetrairon bonding orbitals $(a_1 + e + t_2)$ due to strong π^*(NO) stabilization effects of the π-acidic nitrosyl ligands. The six equivalent electron-pair Fe—Fe bond lengths in $Fe_4(NO)_4(\mu_3\text{-}S)_4$ and in $Fe_4(NO)_4(\mu_3\text{-}Se)_4$ are in complete accordance with the proposed electronic configuration.

In the $Fe_4(CO)_{12}(\mu_3\text{-}X)_4$ tetramers where the neutral CO and X^{2-} ligands generate four d^6 Fe^{II}, the ground-state electronic configuration of the tetrairon orbitals no doubt is similar to that previously determined [11,12] for the $[Fe_4(\eta^5\text{-}C_5H_5)_4(\mu_3\text{-}S)_4]^n$ series due to the generation by the $Fe(CO)_3$ or isolobal $Fe(\eta^5\text{-}C_5H_5)$ fragments of a localized octahedral-like ligand field about each iron atom. This results in the two $3d\sigma$ iron AO's, which transform under molecular T_d symmetry as the eight $(e + t_1 + t_2)$ tetrairon orbitals, being utilized together with the 4s and 4p iron AO's in metal—ligand bonding. Hence, the energy level ordering for the 24 iron core electrons in **1** or **2** is $(a_1 + e + t_2)^{12}(t_1 + t_2)^{12}(e + t_1 + t_2)^0$ in which the filled antibonding tetrairon cluster orbitals $(t_1 + t_2)$ effectively cancel out the filled bonding tetrairon cluster orbitals. The net limiting tetrametal bonding order of zero for **1** and for **2** is consistent with their observed Fe···Fe nonbonding distances.

Alternatively, either **3** or **4** with its completely bonding iron tetrahedron may be depicted as a 60-electron metal-cluster system (composed of four d^7 Fe^I, four six-electron donor X^{2-} ligands, and four two-electron donor NO^+ ligands). This bonding scheme, which essentially book-keeps the composite ligand- and metal-based MO's, may readily be intregrated with the qualitative metal cluster model which considers only the metal-based cluster MO's. For either **3** or **4** the four tetrahedral-like NO^+ and X^{2-} donor orbitals about each iron combine under T_d symmetry to give 16 group donor orbitals of representations $(2a_1 + e + t_1 + 3t_2)$. In turn, these low-energy donor group orbitals are assumed to interact with a similar set of higher-energy tetrairon symmetry orbitals of 4s and 4p iron AO character to give 16 low-energy, filled iron—ligand bonding combinations (of mainly ligand orbital character) and 16 high-energy, empty iron—ligand antibonding combinations (of mostly iron-based character). The 16 filled iron-ligand bonding combinations together with the 14 occupied iron-based MO's (viz., the 8 tetrairon nonbonding ($e + t_1 + t_2$) and 6 tetrairon bonding ($a_1 + e + t_2$) cluster orbitals) make up (under our boundary conditions) the 30 so-called cluster valence molecular orbitals [59] which are used to contain the 60 valence electrons.

Likewise, each of the $Fe_4(CO)_{12}(\mu_3\text{-}X)_4$ tetramers, 1 and 2, may be considered as a 72-electron metal-cluster system (consisting of four d^6 Fe^{II}, four six-electron donor X^{2-} ligands, and twelve CO-electron donor CO ligands. In this instance, the six octahedral-like CO and X^{2-} donor orbitals about each iron transform under T_d symmetry to give 24 group donor orbitals which span the representations ($2a_1 + 2e + 2t_1 + 4t_2$). The interaction of these low-energy donor group orbitals with an analogous group of higher-energy tetrairon symmetry orbitals of 4*s*, 4*p* and 3*d*σ AO character produces 24 low-energy, filled iron—ligand bonding MO's (of principally ligand orbital character) and 24 high-energy, empty iron—ligand antibonding MO's (of mainly iron-based character). Electron-occupation of the 24 iron—ligand bonding MO's as well as of the 6 tetrairon bonding and 6 tetrairon antibonding cluster orbitals gives rise to a 72-electron metal-cluster system which thereby corresponds to a completely nonbonding iron tetrahedron in 1 or 2. It is then apparent from these symmetry considerations that the replacement of the four nitrosyl ligands in the $Fe_4(NO)_4(\mu_3\text{-}X)_4$ precursor by twelve carbonyl ligands in the resulting $Fe_4(CO)_{12}(\mu_3\text{-}X)_4$ tetramer corresponds electronically to a net increase in the Fe_4X_4 core of 12 valence electrons which completely fill the tetrairon antibonding ($t_1 + t_2$) cluster orbitals, thereby changing the total Fe—Fe bond order in the Fe_4X_4 core from six to zero.

Current research has indicated that 1 and 2 can be oxidized to their monocations, with either Br_2 or ICl. It is hoped that the monocation can be crystallized as a suitable salt for an X-ray crystallographic analysis in order to provide a further operational test of the metal cluster bonding model. This scheme predicts that a one-electron oxidation of 1 or 2 to its monocation, by which the electron is removed from a triply degenerate antibonding metal cluster orbital, should result via a first-order Jahn-Teller effect in a distortion of the cubic T_d Fe_4X_4 core to a tetragonal D_{2d} geometry with a relative shortening of either two or four of the six nonbonding Fe···Fe distances. The latter tetragonal distortion was found [49] to occur upon oxidation of the electronically equivalent $Co_4(\eta^5\text{-}C_5H_5)_4(\mu_3\text{-}S)_4$ parent to its monocation.

Stereochemical relationship of 1 and 2 with the $Pt_4Me_{12}(\mu_3\text{-}X)_4$ tetramers, and a structural-bonding analysis of the presumed cubane-like "tetramethylplatinum"

The fact that 1 and 2 are also structurally analogous to the electronically equivalent d^6 Pt^{IV} trimethylplatinum tetramers *, $Pt_4Me_{12}(\mu_3\text{-}X)_4$ [26], such as $Pt_4Me_{12}(\mu_3\text{-}Cl)_4$ [27] and $Pt_4Me_{12}(\mu_3\text{-}OH)_4$ [28—30], brings to the forefront

---

* Solid-state structures have been ascertained from diffraction studies for X = Cl [27], I [60], OH [28—30], and N_3 [61]. In addition the crystal structure of triethylplatinum(IV) chloride, $Pt_4Et_{12}(\mu_3\text{-}Cl)_4$, has been established from X-ray diffraction measurements [62]. These tetramers expectedly have tetrametal-nonbonding Pt_4X_4 cores of idealized cubic T_d architecture.

the case history of "tetramethylplatinum". In 1938 Gilman and Lichtenwalter [31,32] described the preparation and properties of "tetramethylplatinum" which was characterized only by elemental (Pt, C, H) analysis at that time - viz., in the prespectroscopic era before the advent of infrared and NMR spectroscopy as fingerprinting methods. Its presumed structure was analyzed from a partial X-ray diffraction study in 1947 by Rundle and Sturdivant [27] who simultaneously reported the structure of trimethylplatinum chloride which represents the first crystallographically proven example of a cubane-like geometry. Although the coordinates of the methyl carbon atoms were not obtained from the limited photographic X-ray diffraction data for either compound, the crystals (supplied by Professor Henry Gilman of Iowa State University) of the presumed "tetramethylplatinum" compound were found to be isomorphic with those of trimethylplatinum chloride. Hence, on the basis of cubic crystal symmetry (which greatly simplified the structural determination of the chloride tetramer) coupled with the reasonable assumption of octahedral coordination about each Pt^{IV}, a cubane-like $Pt_4Me_{12}(\mu_3\text{-}Me)_4$ tetramer analogous to that of $Pt_4Me_{12}(\mu_3\text{-}Cl)_4$ was formulated by Rundle and Sturdivant [27] who proposed that two electrons were involved in the bonding of each bridging methyl carbon to its three platinum atoms. The probable nonexistence of this compound was later reported in 1968 by Donnay, Cowan, and coworkers [28] and in 1969 by Hoechstetter and Brubaker [33]; convincing evidence (including a comparison of preparative, analytical, and crystallographic data) was put forth [28] that the original compound instead was trimethylplatinum hydroxide in which the postulated bridging methyl groups are in reality hydroxide ligands. The entire crystal structure of this latter cubane-like tetramer, which has been spectroscopically characterized [26,34,35] both in solution and in the solid state, was also ascertained independently in 1968 from three-dimensional X-ray diffraction data [29] and from three-dimensional neutron diffraction data [30].

Electronic considerations based entirely on symmetry arguments reveal that, in spite of no present-day structural example (to our knowledge) of a methyl group coordinated to three metal atoms, the formulated $Pt_4Me_{12}(\mu_3\text{-}Me)_4$ (composed of four d^6 Pt^{IV} and sixteen two-electron donor methyl ligands) may be regarded as an electron-deficient 56-electron cluster which thereby is electronically equivalent to the cubane-like $Re_4(CO)_{12}(\mu_3\text{-}H)_4$ cluster [36—38]. This latter 56-electron tetramer expectedly possesses a completely bonding tetrahedron of rhenium atoms with an average Re—Re distance of 2.91 Å [37], which is significantly shorter than the electron-pair Re—Re distance of 3.02 Å in $Re_2(CO)_{10}$ [63], in accordance with its electronic configuration [38]. It follows that any 56-electron metal-cluster system should possess bonding metal—metal distances. Hence, the fact that the Pt—Pt distance of 3.44 Å reported by Rundle and Sturdivant [27] for the regular platinum tetrahedron in the presumed "tetramethylplatinum" is a nonbonding rather than a bonding value leads us to unambiguous conclusion that their crystals were indeed the previously suggested $Pt_4Me_{12}(\mu_3\text{-}OH)_4$ [28], a 72-electron system with a Pt—Pt distance of 3.430(2) Å [29].

In a sense, it is ironic that a plausible but yet incorrect structure led Rundle and Sturdivant [27] to propose the then unprecedented bonding concept of a four-center, two-electron bond. Furthermore, this work on a presumed novel electron-deficient compound was also the impetus for subsequent stereochemical-bonding studies by Rundle and coworkers [64—66] of two prototype methyl-bridged electron-deficient structures (viz., the trimethylaluminum dimer [65,67] and the dimethylberyllium polymer [66]), from which Rundle [64] developed his widely accepted delocalized bonding model for electron-deficient compounds.

Appendix

Treatment of the stacking fault disorder in 1 and 2 via a scale-factor approach in the least-squares refinement.

(a) General method. When a stacking fault consists of a purely translational displacement of the crystal structure by simple fractions of the unit-cell axes, then the net consequence involves a change in the relative scale of the $|F_0(hkl)|^2$ in certain index classes but not a variation in the relative $|F_0(hkl)|^2$ within a single index class.

If the fault does not upset the coherence of diffraction from a mosaic block in a crystal, it follows for this block that

$$F(S) = \int \sum_N a_N \rho(r) \exp[2\pi i(r - r_N) \cdot S]\, \mathrm{d}V_r$$

where S is the reciprocal lattice scattering vector of magnitude $|S| = 2 \sin \theta/\lambda$, $\rho(r)$ is the scattering density in an unfaulted crystal, r_N ($r_1 \equiv 0$) is the displacement of the crystal structure for the Nth component, and $a_N(\Sigma_N a_N = 1)$ is the relative abundance of the Nth component.

Thus, $F(S) = \sum\limits_N a_N \exp(-2\pi i r_N \cdot S)\, \hat{F}(S)$

where $\hat{F}(S)$ is the value of $F(S)$ should no crystal disorder occur (i.e., $a_1 = 1$, $a_N = 0, N > 1$).

For $|F(S)|^2 = K^2 |\hat{F}(S)|^2$,

one can define

$$K^2 = \sum_M \sum_N a_M a_N \cos[2\pi(r_N - r_M) \cdot S],$$

where $S = ha^* + kb^* + lc^*$ and $r_N - r_M = n_1 a + n_2 b + n_3 c$. If n_1, n_2, n_3 have simple fractions for all N, M, then only a very limited number of K^2 values will occur.

Space group *Bmmb*: $h + l = 2n$ only for $\{hkl\}$. Assume that the stacking fault is I-centering: Then $r_1 = 0$, $r_2 = 1/2(a + b + c)$, $r_3 = 1/2(a + c)$, $r_4 = 1/2b$, and $a_1 = a_3$, $a_2 = a_4$. This gives rise to $K_1^2 = (a_1 + a_2)^2$ for $k = 2n$, $h + l = 2n$ and $K_2^2 = (a_1 - a_2)^2$ for $k = 2n + 1$, $h + l = 2n$ along with $a_2/a_1 = (K_1 - K_2)/(K_1 + K_2)$.

Space group $I4_1/amd$: $h + k + l = 2n$ only for $\{hkl\}$. Assume that the stacking fault can be either B- or A-centering or both. Then $r_1 = 0$, $r_2 = 1/2(a + c)$, $r_3 = 1/2(b + c)$, $r_4 = 1/2(a + b)$, $r_5 = 1/2(a + b + c)$, $r_6 = 1/2\, b$, $r_7 = 1/2\, a$, $r_8 = 1/2\, c$ and $a_1 = a_5$, $a_2 = a_6$, $a_3 = a_7$, $a_4 = a_8$. These relationships lead to $K_1^2 = (a_1 + a_2 + a_3 + a_4)^2$ for $h = 2n$, $k = 2n$, $l = 2n$, $K_2^2 = (a_1 - a_2 - a_3 + a_4)^2$ for $h = 2n + 1$, $k = 2n + 1$, $l = 2n$, $K_3^2 = (a_1 - a_2 + a_3 - a_4)^2$ for $h = 2n$, $k = 2n + 1$, $l = 2n + 1$, and

$K_4^2 = (a_1 + a_2 - a_3 - a_4)^2$ for $h = 2n + 1$, $k = 2n$, $l = 2n + 1$.

(b) Application of the model to 1 and 2 and resulting implications. Expectation values of $\langle K_i^2 \rangle$ have to be obtained in order to evaluate the intensity of each reflection from all of the mosaic blocks of the crystal of **2**. Since *hkl* and *khl* data were merged, this imposed the constraint $\langle K_3^2 \rangle = \langle K_4^2 \rangle$ so that $\langle a_2^2 \rangle = \langle a_3^2 \rangle$. Since the above four equations give rise to the relationship $\langle K_2^2 \rangle = \langle K_3^2 \rangle + \langle K_4^2 \rangle - \langle K_1^2 \rangle + 8\langle a_2 a_3 \rangle + 8\langle a_1 a_4 \rangle$ (1), it follows that if coherence within a mosaic block can be maintained for more than parallel stacking faults (i.e., $\langle a_2 a_3 \rangle$ and $\langle a_1 a_4 \rangle$ are nonzero), it should be evidenced by the value of $\langle K_2^2 \rangle$ being significantly greater than $\langle K_3^2 \rangle + \langle K_4^2 \rangle - \langle K_1^2 \rangle$. However, least-squares refinement of **2** with K_1, K_2, and $K_3 = K_5$ as independent scale factors showed that this was not so. (In fact, should the inequality hold strongly, it is reasonable to assume that K_2, K_3, and K_4 would approximate zero). This incompatibility of the experimental data with the above model suggested that within a single mosaic block the stacking fault is B-centered (i.e., corresponding to the B-centered orthorhombic lattice of **1**) such that $\langle a_2 a_3 \rangle = \langle a_1 a_4 \rangle = 0$. The above scale-factor relation ships of $\langle K_1^2 \rangle + \langle K_2^2 \rangle = \langle K_3^2 \rangle + \langle K_4^2 \rangle$ and $\langle K_3^2 \rangle = \langle K_4^2 \rangle$ then lead to $\langle K_3^2 \rangle = (\langle K_1^2 \rangle + \langle K_2^2 \rangle)/2$, which reduces the number of independent scale-factor variables to K_1 and K_2 (i.e., one additional parameter over the single scale factor normally utilized in the refinement of a completely ordered structure). This resulting model for **2**, which is a physically reasonable one in involving only parallel-stacking faults in a mosaic component of a crystal, gives rise to the relationships $K_1^2 = (a_1 + a_2)^2$, $K_2^2 = (a_1 - a_2)^2$, $(K_3^2 + K_4^2)/2 = a_1^2 + a_2^2$, and $a_2/a_1 = (K_1 - K_2)/(K_1 + K_2)$ for least-squares refinement.

There are distinct advantages in varying scale factors rather than occupancy factors in a refinement of a crystal structure possessing stacking faults. Equal-molecule constraints are easily maintained as no conditions need to be imposed either on occupancy factors or on positional and/or thermal parameters in order to make the refinement behave. Secondly, from a determination of the scale factors F_0 and F_c data can be reconstituted on an absolute scale to produce Fourier maps where the effects of the crystal disorder are removed. Thirdly, only the atomic positions of the ordered structure need be included in the refinement. It should be noted that in order to refine the disordered model correctly for the $I4_1/amd$ crystal with a single scale factor, it would have been necessary to describe the crystal as having twinned orthorhombic components. Each component would be the same orthorhombic structure corresponding to a B-centered fault imposed on $I4_1/amd$. The twinning would impose the interchange of the *a* and *b* axial directions, thus superimposing $|F(hkl)|^2$ and $|F(khl)|^2$ in order to maintain the observed D_{4h} Laue symmetry for the intensity-weighted reciprocal lattice. One could then extract phase information for a Fourier map from the relationship $|F_0(hkl)|/|F_0(khl)| = |F_c(hkl)|/|F_c(khl)|$ in which the observed intensity is partitioned into $|F_0(hkl)|$ and $|F_0(khl)|$ and given the phase of $F_c(hkl)$ and $F_c(khl)$, respectively. One would then obtain an electron-density map of the disordered crystal structure but with the artifacts of the twinning removed. These artifacts affect the apparent occupancies of atoms within disordered molecules.

Acknowledgments

This research was supported by a grant from the National Science Foundation. We are indebted to Mr. Dick A. Nagaki (UW-Madison) for mass spectroscopic measurements and to Mr. Mark H. Englert (UW-Madison) for magnetic susceptibility measurements. One of us (L.F.D.) would like to express his deep appreciation for being able to contribute to this series honoring the professional achievements of Professor Henry Gilman. The pioneering work of his research group at Iowa State University in organometallic chemistry has had a tremendous impact in laying its foundations and in providing the stimulus for much present-day work. His inspiration for working hard in the laboratory and his devotion to chemistry were special ingredients which were evident from an informal association with his group during my graduate carreer at Iowa State as a professional son of the late Professor Robert E. Rundle.

References

1 T.H. Lemmen, J.A. Kocal, F.Y.-K. Lo, M.W. Chen, and L.F. Dahl, J. Amer. Chem. Soc., 103 (1981) 1932, and references cited therein.
2 C.T.-W. Chu, R.S. Gall, and L.F. Dahl, J. Amer. Chem. Soc., in press.
3 C.T.-W. Chu, F.Y.-K. Lo, and L.F. Dahl, submitted for publication.
4 R.S. Gall, C.T.-W. Chu, and L.F. Dahl, J. Amer. Chem. Soc., 96 (1974) 4019.
5 L.L. Nelson and L.F. Dahl, to be published.
6 L.L. Nelson and L.F. Dahl, to be published.
7 A.S. Foust and L.F. Dahl, J. Amer. Chem. Soc., 92 (1970) 7337.
8 A.R. Rae, RAELS, A comprehensive Least-Squares Program, University of New South Wales, Kensington, 1976; Adapted for a Harris/7 computer by A.D. Rae, University of Wisconsin-Madison, 1980.
9 R.A. Schunn, C.J. Fritchie, Jr., and C.T. Prewitt, Inorg. Chem., 5 (1966) 892..
10 C.H. Wei, G.R. Wilkes, P.M. Treichel, and L.F. Dahl, Inorg. Chem., 5 (1966) 900.
11 Trinh-Toan, W.P. Fehlhammer, and L.F. Dahl, J. Amer. Chem. Soc., 99 (1977) 402.
12 Trinh-Toan, B.K. Teo, J.A. Ferguson, T.J. Meyer, and L.F. Dahl, J. Amer. Chem. Soc., 99 (1977) 408.
13 B.A. Averill, T. Herskovitz, R.H. Holm, and J.A. Ibers, J. Amer. Chem. Soc., 95 (1973) 3523.
14 L. Que, Jr., M.A. Bobrik, J.A. Ibers, and R.H. Holm, J. Amer. Chem. Soc., 96 (1974) 4168.
15 M.C. Carrell, J.P. Glusker, R. Job, and T.C. Bruice, J. Amer. Chem. Soc., 99 (1977) 3683.
16 E.J. Laskowski, R.B. Frankel, W.O. Gillum, G.C. Papaefthymiou, J. Renaud, J.A. Ibers, and R.H. Holm, J. Amer. Chem. Soc., 100 (1978) 5322.
17 E.J. Laskowski, J.G. Reynolds, R.B. Frankel, S. Foner, G.C. Papaefthymiou, and R.H. Holm, J. Amer. Chem. Soc., 101 (1979) 6552.
18 J.M. Berg, K.O. Hodgson, and R.H. Holm, J. Amer. Chem. Soc., 101 (1979) 4586.
19 M.A. Bobrik, K.O. Hodgson, and R.H. Holm, Inorg. Chem., 16 (1977) 1851.
20 J.A. Ibers and R.H. Holm, Science, 209 (1980) 223, and references cited therein.
21 D. Bright, J. Chem. Soc. Chem. Commun., (1970) 1169.
22 E. Horn and M.R. Snow, Aust. J. Chem., XX (1981) XXX.
23 E. Rottinger and H. Vahrenkamp, Angew. Chem. Int. Ed. Engl., 17 (1978) 273.
24 E. Horn, M.R. Snow, and P.C. Zeleny, Aust. J. Chem., 33 (1980) 1659.
25 W. Harrison, W.C. Marsh, and J. Trotter, J. Chem. Soc. Dalton Trans., (1972) 1009.
26 T.G. Appleton and J.R. Hall, Aust. J. Chem., 33 (1980) 2387, and references cited therein.
27 R.E. Rundle and J.H. Sturdivant, J. Amer. Chem. Soc., 69 (1947) 1561.
28 G. Donnay, L.B. Coleman, N.G. Krieghoff, and D.O. Cowan, Acta Cryst. B, 24 (1968) 157.
29 T.G. Spiro, D.H. Templeton, and A. Zalkin, Inorg. Chem., 7 (1968) 2165.
30 H.S. Preston, J.C. Mills, and C.H.L. Kennard, J. Organometal. Chem., 14 (1968) 447.
31 H. Gilman and M. Lichtenwalter, J. Amer. Chem. Soc., 60 (1938) 3085.
32 H. Gilman, M. Lichtenwalter, and R.A. Benkeser, J. Amer. Chem. Soc., 75 (1953) 2063.
33 M.N. Hoechstetter and C.H. Brubaker, Jr., Inorg. Chem., 8 (1969) 400.
34 G.L. Morgan, R.D. Rennick, and C.C. Soong, Inorg. Chem., 5 (1966) 372.
35 P.A. Bulliner, V.A. Maroni, and T.G. Spiro, Inorg. Chem., 9 (1970) 1887, and references cited therein.
36 R. Saillant, G. Barcelo, and H.D. Kaesz, J. Amer. Chem. Soc., 92 (1970) 5739.

37 R.D. Wilson and R. Bau, J. Amer. Chem. Soc., 98 (1976) 4687.
38 R. Hoffmann, B.E.R. Schilling, R. Bau, H.D. Kaesz, and D.M.P. Mingos, J. Amer. Chem. Soc., 100 (1978) 6088.
39 L.R. Byers and L.F. Dahl, Inorg. Chem., 19 (1980) 277.
40 International Tables for X-ray Crystallography, Vol. IV, Kynoch Press, Birmingham, England, 1974, pp. 148—150.
41 P. Main, L. Lessenger, M.M. Woolfson, G. Germain, and J.-P. Declercq, MULTAN-76, an updated version of MULTAN, G. Germain, P. Main, and M.M. Woolfson, Acta Crystallogr., A, 27 (1971) 368.
42 J. Waser, Acta Crystallogr., 16 (1963) 1091.
43 A.D. Rae, Acta Crystallogr. A, 34 (1978) 578.
44 W.R. Busing, K.O. Martin, and H.A. Levy, OR FLS, ORNL-TM-305, Oak Ridge National Laboratory, Oak Ridge, Tennessee, 1962.
45 A.D. Rae, Acta Crystallogr. A, 31 (1975) 560.
46 W.R. Busing, Acta Crystallogr. A, 27 (1971) 683.
47 F.A. Cotton and J.M. Troup, J. Chem. Soc. Dalton Trans., (1974) 800.
48 V. Albano, P. Bellon, G. Ciani, and M. Manassero, J. Chem. Soc. Chem. Commun., (1969) 1242.
49 G.L. Simon and L.F. Dahl, J. Amer. Chem. Soc., 95 (1973) 2164.
50 C.R. Szmanda and L.F. Dahl, to be published.
51 R.E. Johnson and L.F. Dahl, to be published.
52 H.-J. Haupt, F. Neumann, and H. Preut, J. Organometal. Chem., 99 (1975) 439.
53 G.L. Simon and L.F. Dahl, J. Amer. Chem. Soc., 95 (1973) 2175.
54 Trinh-Toan, Ph.D. Thesis, University of Wisconsin-Madison, 1972.
55 B.K. Teo, Ph.D. Thesis, University of Wisconsin-Madison, 1973.
56 B.K. Teo, C.R. Szmanda, and L.F. Dahl, to be published.
57 C.F. Campana, T.F. Block, and L.F. Dahl, to be published.
58 M.B. Hall and R.F. Fenske, Inorg. Chem., 11 (1972) 768.
59 J.W. Lauher, J. Amer. Chem. Soc., 100 (1968) 5305.
60 G. Donnay, L.B. Coleman, N.G. Krieghoff, and D.O. Cowan, Acta Crystallogr. B, 24 (1968) 157.
61 M. Atam and U. Müller, J. Organometal. Chem., 71 (1974) 435.
62 R.N. Hargreaves and M.R. Truter, J. Chem. Soc. (A), (1971) 90.
63 L.F. Dahl, E. Ishishi, and R.E. Rundle, J. Chem. Phys., 26 (1957) 1750.
64 R.E. Rundle, J. Phys. Chem., 61 (1957) 45, and references cited therein.
65 P.H. Lewis and R.E. Rundle, J. Chem. Phys., 21 (1953) 986.
66 A.I. Snow and R.E. Rundle, Acta Cryst., 4 (1951) 348.
67 R.G. Vranka and E.L. Amma, J. Amer. Chem. Soc., 89 (1967) 3121.